MULTI-METHOD GEOPHYSICAL EXPLORATION OF THE MCMINN COUNTY AIRPORT

Kevin D. Hon, P.G., Geophysical Group Leader
S&ME, Inc.
Chattanooga, Tennessee, USA
email: khon@smeinc.com - Corresponding Author

Jason B. Cox, P.G., Project Geophysicist
S&ME, Inc.
Charlotte, North Carolina, USA
email: jcox@smeinc.com

Introduction

Sinkholes have been forming for several years in the northern portion of the McMinn County Airport located southeast of Athens, Tennessee. Repairs to the sinkholes had typically been conducted by the county at the time of their occurrence, however, the rate of occurrences significantly increased and included several that formed adjacent to previously repaired sinkholes. As such, geophysical services were conducted at the site in order to identify possible trends and/or anomalous features within the underlying soil and bedrock that may be related to karst conditions. The geophysics provided a cost effective means to assist in developing a geotechnical boring program for determining possible steps for remediation. The utilized geophysical methods consisted of ground penetrating radar (GPR), electrical resistivity tomography (ERT), and spontaneous potential (SP).

At the time of our initial site visits in late 2014, and again in early 2015, there were approximately 10 depressions clustered around the taxiway area, which included one that had recently developed in the middle of the taxiway resulting in damage to a small plane. Size of the depressions ranged from about 10 to 20 feet in diameter and up to about 10 feet in depth. Most of the sinkholes formed after large rain events along an unlined drainage ditch located west of the taxiway (Figures 1 through 3). However, several isolated depressions/sinkholes have also occurred in recent years in other areas of the northern portion of the airport. Sinkhole activity along the drainage ditch and taxiway continued, and actually increased, throughout the course of our exploration. The only potential indication of karst activity associated with the runway is a slight dip about 50 feet wide located along the western edge of the pavement.

Keywords: Karst, Sinkhole, Airport, Geotechnical, Ground Penetrating Radar, Electrical Resistivity Tomography, Spontaneous Potential.

Figure 1: Sinkholes adjacent to taxiway (Google Earth Pro images dated 10/14/2015).

Figure 2: Sinkholes adjacent to and within taxiway (view to the east).

Figure 3: Sinkholes adjacent to taxiway along drainage ditch (view to the south).

There are two large depressions that lie to the east and west of the airport that currently serve as drainage basins to the surrounding area; the one to the west of the site actually encompasses about 50 acres. The majority of the sinkholes that have formed on the property lie in-between these two areas, which are only about 600 to 700 feet away from the cluster. Based on aerial photographs and topo maps, there are other depressions outside of the property that appear to align with the sinkholes that have developed at the site (Figure 4). In addition, the sinkhole activity is located within the portion of the airport that was expanded several years ago. The approximate 2,000 foot runway expansion required the removal of up to about 30 feet of overburden during construction (Figure 5).

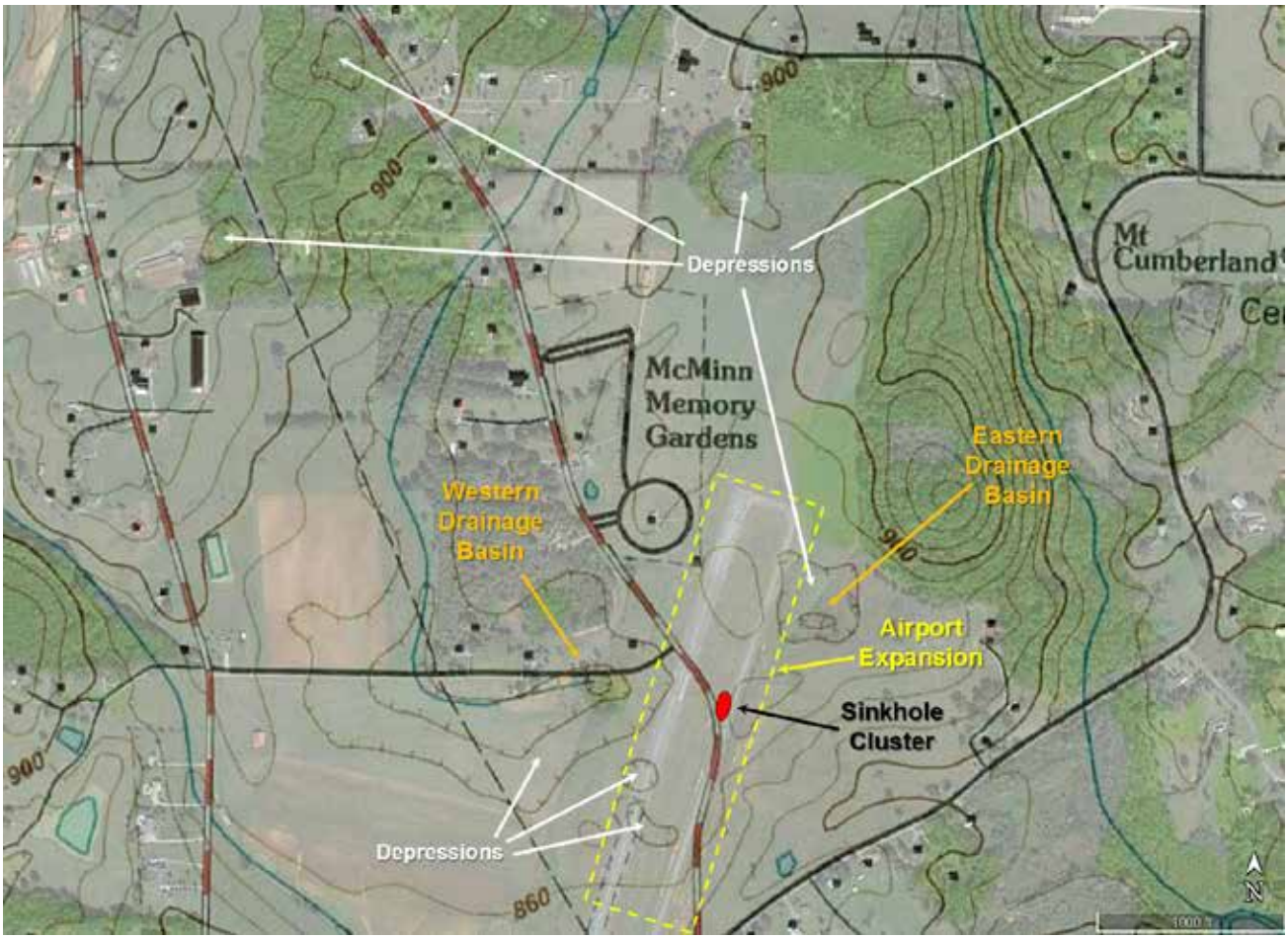

Figure 4: Depression location map (Google Earth Pro image with U.S. Geological Survey historical topographic map overlay; Athens, TN, 1:24,000 quad, 1964).

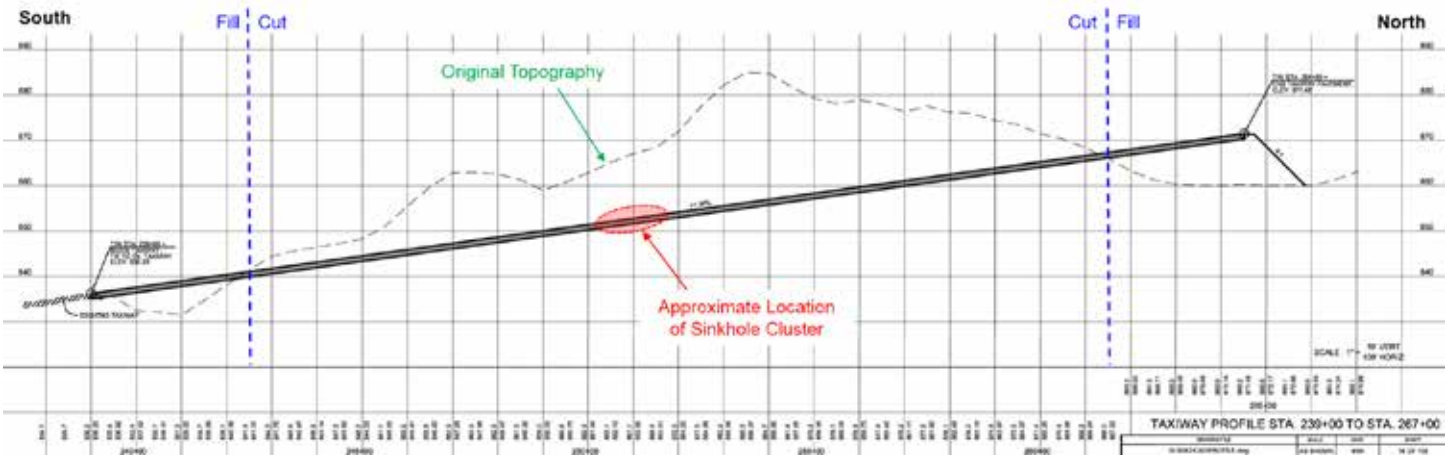

Figure 5: Taxiway expansion grading profile.

Geologic Background

Athens, Tennessee is located in the Appalachian Valley and Ridge Physiographic Province which is characterized by elongated ridges that trend in a northeast-southwest direction. The ridges are typically formed on highly resistant sandstones and shales, while the valleys and rolling hills are formed on less resistant limestone, dolomite, and shales (Safford, 1869). The Kingsport Formation of the Knox Group underlies the site and generally consists of siliceous dolomite that usually weathers to form a thick cherty clay overburden (Rodgers, 1953). Of significant importance is also the Chestuee fault, located along the eastern boundary of the project site, as it is common for sinkholes to form near faults and contacts between geologic units in this physiographic province (Figure 6).

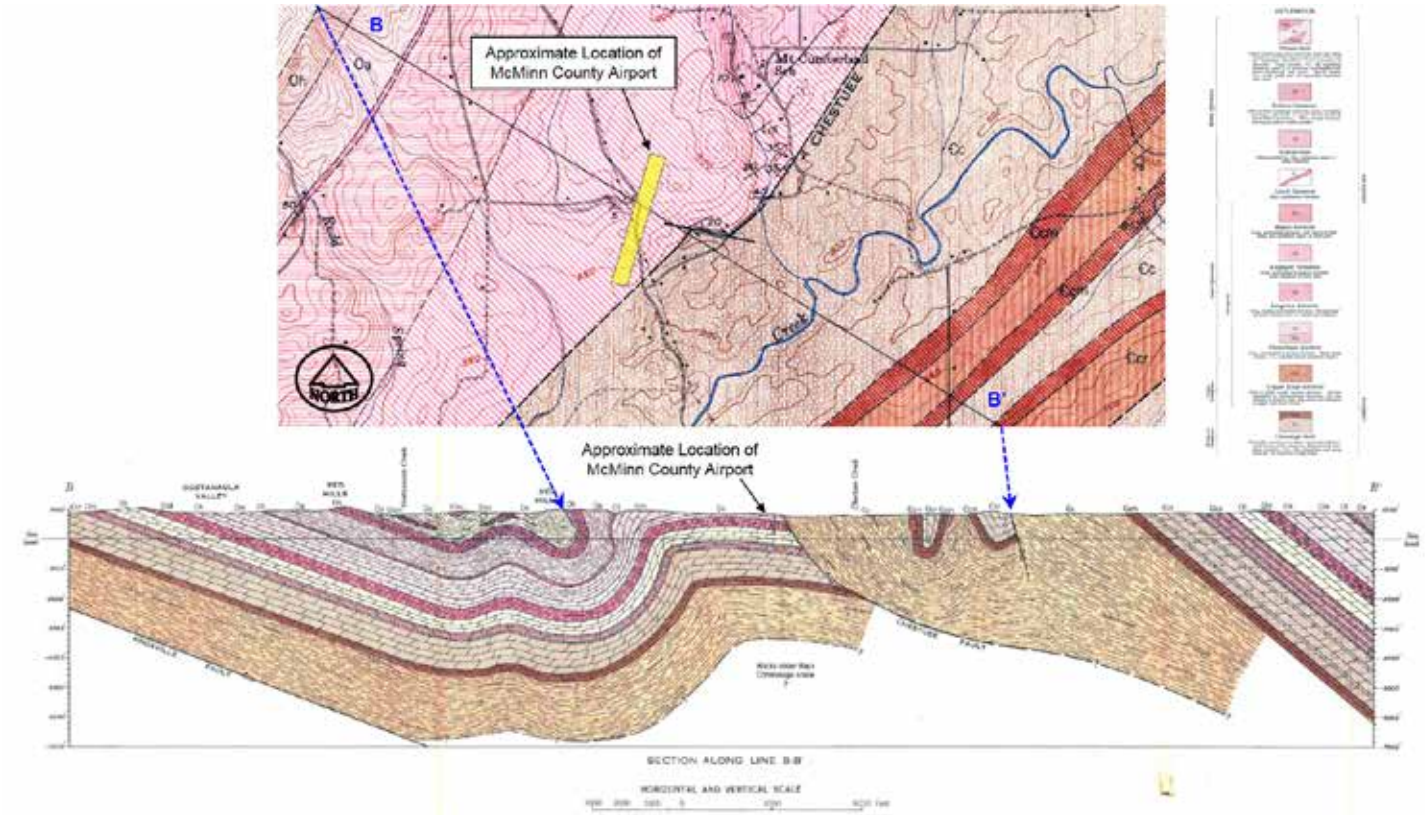

Figure 6: Geologic map and cross-section (Rodgers, 1952).

The dolomite bedrock underlying this site has likely been subject to solution weathering by water percolating downward through the soil and into cracks and fissures gradually dissolving the rock, which produces insoluble impurities such as chert and clay. Since dolomites vary greatly in their resistance to weathering, the soil/bedrock contact tends to be extremely irregular. More soluble bedrock develops a thicker soil cover and a more irregular bedrock surface with pinnacles and slots (Figure 7). Less soluble bedrock usually develops a thinner soil cover and a less irregular soil-bedrock surface. These large variations in bedrock depth are greatly enhanced by the presence of fractures, bedding planes and faults which provide an increased opportunity for a greater influx of percolating water, and hence, a greater potential of sinkhole activity. The weaknesses may form clay-filled cavities or enlarge into caves which can be connected by a network of passageways. If a cave forms close to the bedrock surface, its roof may collapse and the overlying soils may erode into the cave. Once the weight of the overlying soil exceeds the soil's arching strength, the soil collapses and an open hole or depression may appear at the ground surface (Sowers, 1996; Figure 8).

Figure 7: Irregular/pinnacled bedrock exposed within the area of the sinkhole cluster during the current remediation portion of the project (view to the south).

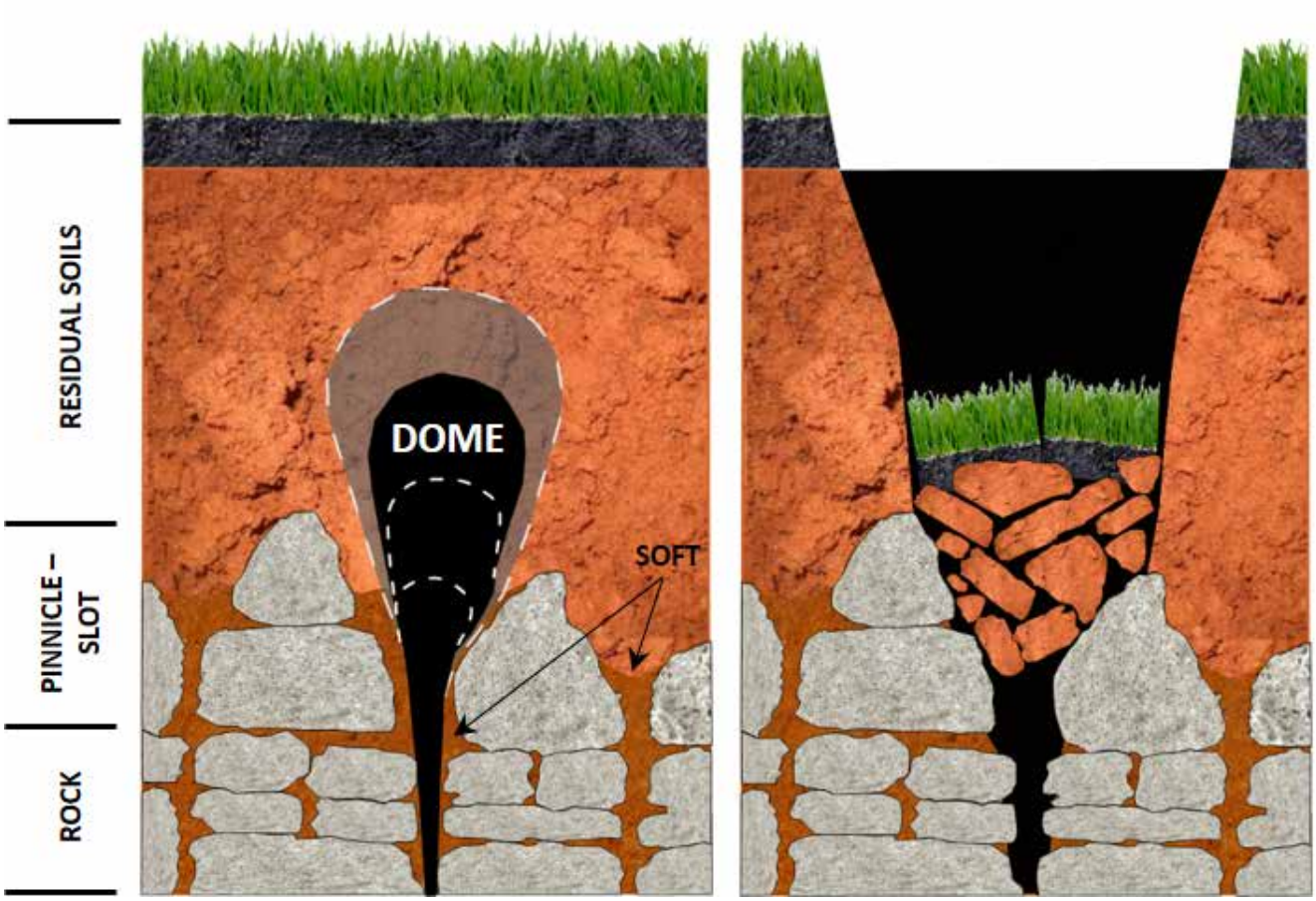

Figure 8: Sinkhole diagrams (modified from Sowers, 1996).

Geophysical Methodology and Field Testing

Variability in the subsurface can be better determined through the implementation of a geophysical survey either prior to a drilling program or in support of a site that has already been drilled. As such, GPR, ERT and SP surveys were employed at the site as an initial phase prior to a geotechnical boring program. A test location plan for the geophysical profile locations is presented in Figure 9.

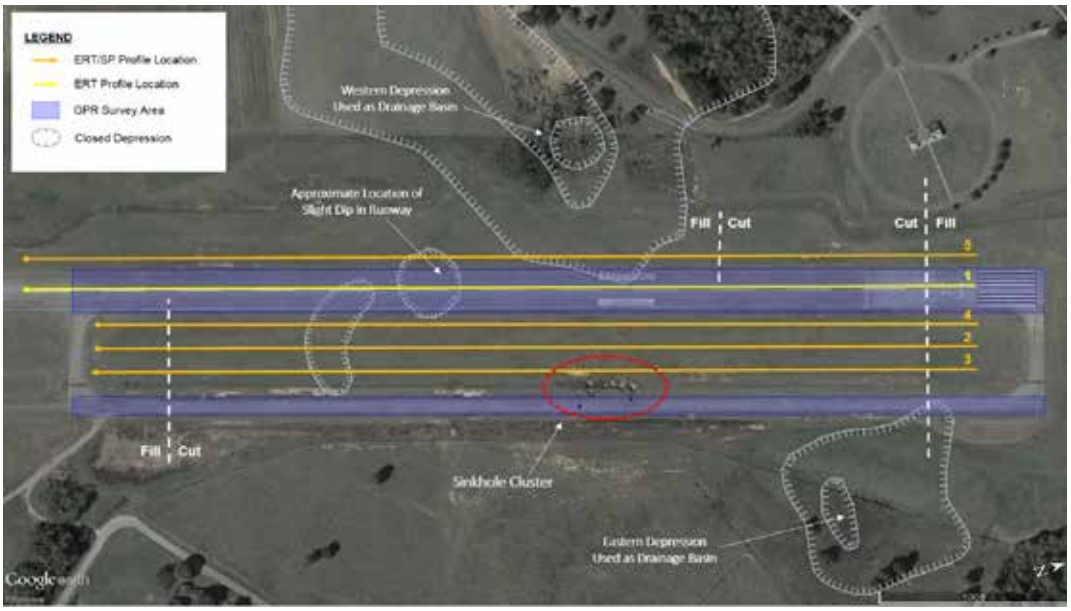

Figure 9: Geophysical test location plan (Google Earth Pro image dated 10/14/2015).

Ground Penetrating Radar

GPR has limited use in clayey soils which are prevalent at this particular site; however, it can be highly effective for use in identifying features and/or voids directly beneath pavements. A Geophysical Survey Systems, Inc. (GSSI) RoadScan 30 system equipped with a 2 GHz horn antenna directly attached to the back of a vehicle was used for the GPR survey (Figure 10). A distance measuring interval (DMI) encoder attached to the vehicle tires was used for triggering the GPR signal and to have a distance reference. Data were acquired every 3 inches at a relatively constant speed of about 20 miles per hour. Sub-meter GPS support was also obtained at 1 second intervals to simultaneously reference the data. GPS positioning is automatically interpolated as necessary. A total of sixteen parallel GPR profiles totaling about 35,000 linear feet were collected in the north to south direction. Spacing between profiles were about 20 feet along the runway and about 10 feet along the taxiway. The GPR survey areas are presented in Figure 9. The depth of signal penetration is a function of the conductivity of the subsurface materials and antenna frequency. Antenna frequency also determines the capable resolution of a potential target. The 2 GHz antenna provides very high resolution but at a maximum penetration depth of about 2 feet below ground surface. The GPR data was processed using the GSSI Radan 7 software package with RoadScan Module.

Figure 10: Photo of GPR system adjacent to sinkhole in taxiway (view to the north).

Electrical Resistivity Tomography

The ERT method is conducive for clayey environments and was used at the site in order to help characterize the lateral changes in subsurface materials with particular focus on potential sinkhole/karst activity. An Advanced Geosciences, Inc. (AGI) SuperSting R8 resistivity meter configured with an 84-channel switchbox, cables and stainless steel electrodes was used for the ERT survey (Figure 11). A total of five profiles ranging between about 1,900 feet and 2,300 feet in length were collected at the site (Figure 9); including one along the middle of the runway which required drilling down through the existing pavement structure and into the underlying soils. Electrodes were spaced at 10 feet and data was collected using the Dipole-Dipole array configuration for each profile. Lighting and grounding systems located adjacent to the runway and taxiway produced extensive noise in test data, so each of the ERT profiles were collected 50 feet or more from these buried structures. These sources of influence unfortunately limited the ability to collect data relatively close to the sinkhole cluster (i.e. adjacent to the taxiway). Two-dimensional profiles were processed using AGI's EarthImager 2D software and Golden Software's Surfer (v. 12.0) was used to grid and plot the data. Elevations for the ERT models were based on provided grading plans.

Figure 11: Photo of ERT layout located east of the runway (view to the north).

Spontaneous Potential

An SP survey was primarily performed in order to identify potential connectivity between the drainage basin depressions located to the east and west of the site. The SP method is a passive electrical technique that involves measurement of naturally occurring "streaming" potentials due to movement of water through porous subsurface media. SP measurements are made using a pair of non-polarizing "porous pot" electrodes (a base and roving electrode) which contain a copper electrode immersed in a saturated copper sulphate solution. The potential difference between the two electrodes is measured using a high impedance voltmeter. Areas of fluid entry and/or downward infiltration generally appear as low voltage anomalies while zones where fluid is migrating upwards are generally higher voltage anomalies.

A total of four SP data profiles were collected using a Fluke 179 Multimeter along the ERT lines collected in the grassy areas as shown in Figure 9 (ERT Lines 2 through 5). SP data were however collected twice; once during a relatively dry period and once right after a period of heavy rain in order to identify potential variances due to an influx of surplus groundwater into the underlying hydrologic system. The "base" electrode was positioned at the northern end of each profile while moving the second "roving" electrode in 10-foot increments towards the south. The two SP data sets for each line were normalized and the Golden Software Surfer (v. 12.0) program was used to present plotted profiles.

Geophysical Results

Several anomalous subsurface features were identified by the geophysical surveys performed at the site and the approximate locations of the most noteworthy features are illustrated in Figure 12. Results for each of the various methods are presented in the following paragraphs.

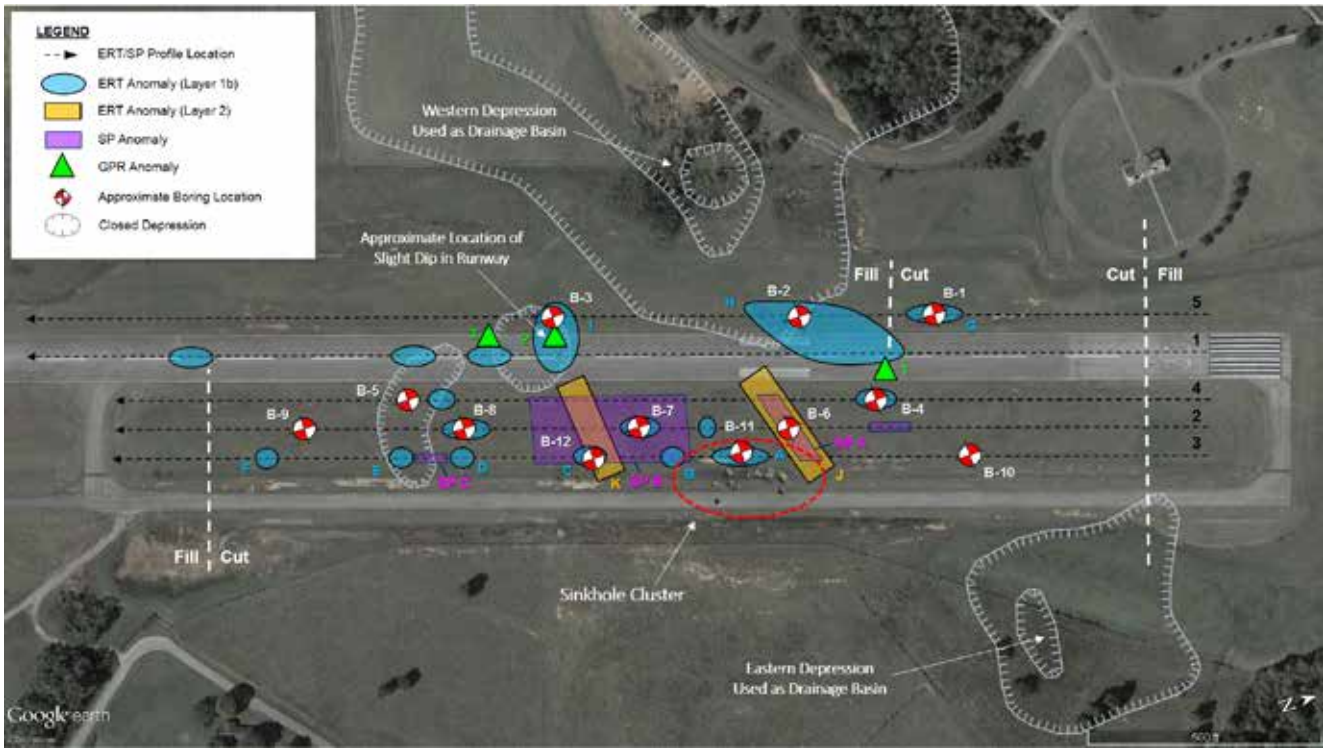

Figure 12: Anomaly location plan (Google Earth Pro image dated 10/14/2015).

Ground Penetrating Radar

Reflections indicative of potential voids were not identified in the GPR data collected at the site. However, three GPR anomalies characterized by relatively small dips/thickening within the underlying stone layers were observed along the runway (GPR Anomalies 1, 2 and 3; Figures 12 and 13). GPR Anomaly 2 is actually located within the slightly depressed area along the western edge of the runway. Since the overlying asphalt appears to be fairly horizontal in these three areas, the variations in the stone may be related to site grading or possible settlement of the stone interval during construction, which could include karst activity.

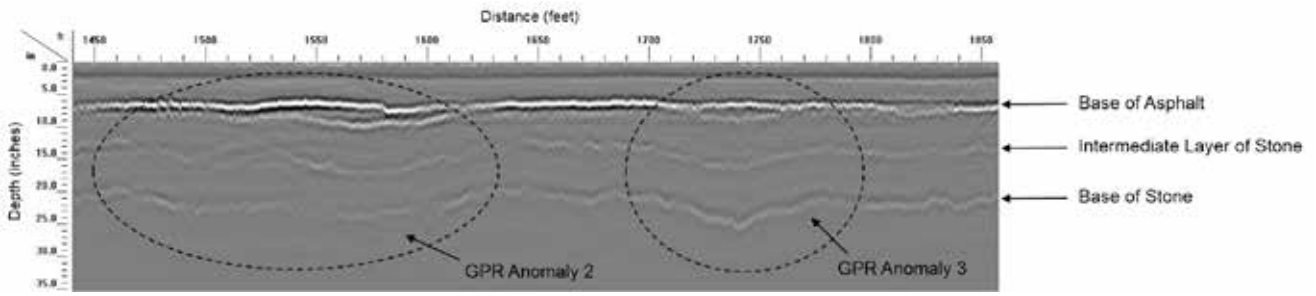

Figure 13: Example GPR profile.

Electrical Resistivity Tomography and Spontaneous Potential

The ERT results indicated a varying resistivity contrast across the surveyed areas typically ranging from about 25 ohm-meters (ohm/m) to 2,500 ohm/m. ERT profile depths are about 80 to 100 feet. Based on geotechnical borings performed at the site, the subsurface conditions generally consist of two layers (Layer 1 and Layer 2). Layer 1 soils range between firm to very soft consistencies and can also be further categorized into three additional zones (Layers 1a, 1b and 1c). Brief descriptions of each interpreted layer are presented in Table 1.

Table 1. Interpreted layer descriptions.

Layer	Average Resistivity Range	Geologic Description
1a	< 500 ohm/m	Relatively conductive layer that consists of lean SILTY CLAY (CL) and FILL with a relatively low concentration of chert fragments
1b	> 500 ohm/m	Resistive layer that ranges between about 20 and 40 feet in thickness and generally corresponds to lean SILTY CLAY (CL) to CLAYEY SILT (ML) with a relatively higher concentration of chert fragments
1c	< 500 ohm/m	Relatively conductive layer that consists of fat SILTY CLAY (CH) with some lean SILTY CLAY (CL) and traces of chert fragments
2	> 500 ohm/m	Resistive layer with an undulating upper boundary that is related to the underlying dolomite

Several prominent anomalous subsurface features were identified in the ERT data sets which can be further categorized as either shallow or deep. The shallow anomalies are characterized by discontinuities in Layer 1b and could be related to previous downward migration of the Layer 1b soils from karst conditions (example Anomalies A through H; Figures 14a-14d). The deep anomalies are characterized by conductive zones within Layer 2 that are also generally associated with topographic lows/depressions along the interpreted top of rock (example Anomalies I and J; Figures 14c and 14d). These deeper anomalies may be related to karst features such as deep soil slots between rock pinnacles and/or fracture zones within the bedrock. Several of the geotechnical borings identified some of these features. In addition, some of the ERT anomalies appear to correspond with depressions identified on topographic maps, within the slightly depressed area along the western edge of the runway, and adjacent to GPR anomalies (Figures 12 and 13). Example ERT data is presented in Figure 14 in which the interpreted layer boundaries, top of bedrock, and anomalies are also illustrated. In addition, the approximate location of adjacent borings were superimposed on the example profiles.

The SP data sets collected at the site ranged from approximately -100 millivolts (mV) to 50 mV, and in general, the two data sets correlated well across each profile. A few potential anomalous responses (positive and negative) were identified and three examples are presented in Figure 14e (SP Anomalies A though C). SP Anomaly A is a positive response identified during both wet and dry conditions with a slight increase during the wet period and may be related to ERT Anomaly I. SP Anomaly B is a broad positive response that also showed a slight increase during the wet period and may be related to ERT Anomaly J. SP Anomaly C is a negative response only identified in the data set collected during the wet period but it does not appear to be associated with any specific ERT anomaly or any observable feature at the site.

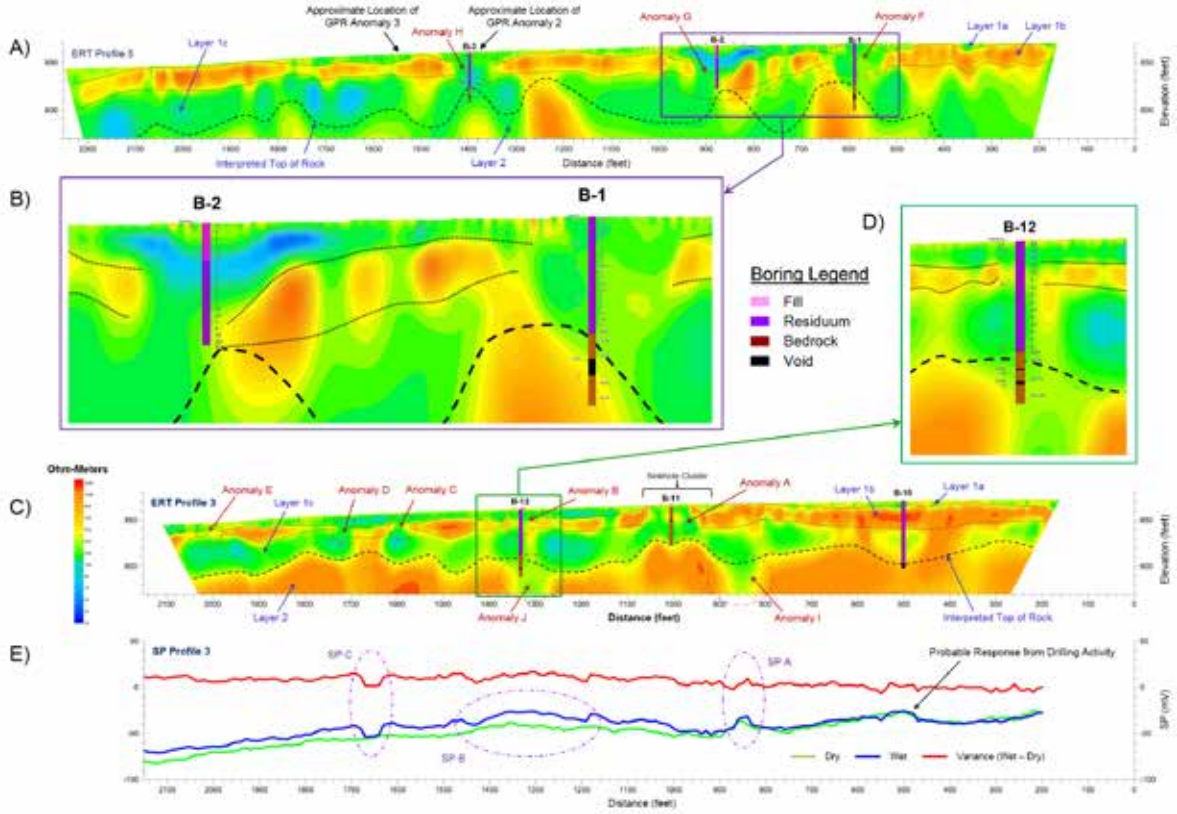

Figure 14: Example geophysical data: (**A**) ERT Profile 5 highlighting prominent observed anomalous features; (**B**) close up view of Anomalies G and F with geotechnical boring overlays; (**C**) ERT Profile 3 highlighting prominent observed anomalous features; (**D**) close up view of Anomalies B and J with geotechnical boring overlays; and (**E**) SP Profile 3 highlighting anomalous features

Conclusions

Guided by the results of the geophysical survey, the geotechnical boring program was able to more accurately identify and confirm the extent of the underlying karst conditions at the site. In all but two control borings performed in areas where the geophysical data did not indicate karst activity, epikarst soils (very soft soil and weathered rock) associated with sinkhole development and/or conditions indicative of solution activity within the bedrock were encountered. Although karst activity at the site was likely expedited due to the removal of the overburden during construction and the introduction of water into the hydrologic system from the unlined drainage ditches paralleling the taxiway (no ditches are located adjacent to the runway), complete elimination of future sinkhole activity is likely not possible considering the extent of the karst activity and the depth to bedrock. However, repairs to the existing sinkholes are currently underway and measures to reduce the frequency of sinkhole formation near the runway and taxiway are planned by controlling surface water runoff and preventing its collection in ditches adjacent to the airport structures.

References

Rodgers, J., 1952, Geologic Map of the Athens Quadrangle, Tennessee, scale 1:24,000.

Rodgers, J., 1953, Geologic Map of East Tennessee with Explanatory Text, Part II: Tennessee Division of Geology, 168 p.

Safford, J. M., 1869, Geology of Tennessee: Nashville, Tennessee, 550 p.

Sowers, G.F., 1996, Building on Sinkholes; Design and Construction of Foundations in Karst Terrain, ASCE Press, 202 p.